IOPscience iopscience.iop.org

Home Search Collections Journals About Contact us My IOPscience

An Au/Si hetero-nanorod-based biosensor for *Salmonella* detection

This article has been downloaded from IOPscience. Please scroll down to see the full text article.

2008 Nanotechnology 19 155502

(http://iopscience.iop.org/0957-4484/19/15/155502)

View the table of contents for this issue, or go to the journal homepage for more

Download details:
IP Address: 129.97.58.73
The article was downloaded on 06/09/2013 at 12:38

Please note that terms and conditions apply.

Nanotechnology **19** (2008) 155502 (7pp) doi:10.1088/0957-4484/19/15/155502

# An Au/Si hetero-nanorod-based biosensor for *Salmonella* detection

**Junxue Fu[1], Bosoon Park[2], Greg Siragusa[2], Les Jones[3], Ralph Tripp[3], Yiping Zhao[1] and Yong-Jin Cho[4]**

[1] Physics and Astronomy Department, University of Georgia, Athens, GA 30602, USA
[2] USDA, ARS, Russell Research Center, Athens, GA 30605, USA
[3] Department of Infectious Diseases, College of Veterinary Medicine, University of Georgia, Athens, GA 30602, USA
[4] Korea Food Research Institute, Songnam, Republic of Korea

E-mail: zhaoy@physast.uga.edu

Received 19 October 2007, in final form 1 February 2008
Published 11 March 2008
Online at stacks.iop.org/Nano/19/155502

**Abstract**
We present a novel and effective food-borne bacteria detection method. A hetero-structured silicon/gold nanorod array fabricated by the glancing angle deposition method is functionalized with anti-*Salmonella* antibodies and organic dye molecules. Due to the high aspect ratio nature of the Si nanorods, dye molecules attached to the Si nanorods produce an enhanced fluorescence upon capture and detection of *Salmonella*. This bio-functional hetero-nanorod detection method has great potential in the food safety industry as well as in biomedical diagnostics.

M Supplementary data are available from stacks.iop.org/Nano/19/155502

(Some figures in this article are in colour only in the electronic version)

## 1. Introduction

*Salmonella* is one of the major causes of bacterial gastroenteritis in humans and a source of many food-related outbreaks, thus rapid and sensitive detection is important in the control of food safety. Various analytical methods have been developed to detect the *Salmonella.* The conventional microbiological technique, i.e. ISO method 6579, often requires up to 5–7 days to obtain a positive result [1–4]. These culture methods have been reported to show poor sensitivity for low-level contamination in samples [5]. To further improve the detection sensitivity, a number of investigators use fluorescent-antibody (FA) procedures for *Salmonella* detection [6–10]. Although FA procedures require less time and have higher sensitivity for detection over culture methods, the detection is still limited by the requirement for substantial numbers of bacteria present for detection to discriminate a fluorescent signal over background fluorescence. This is a relevant issue in food microbiology because the *Salmonella* numbers are usually low, thus it is often necessary to use enrichment culture techniques prior to immunofluorescence microscopy. Therefore the FA procedure in the detection of *Salmonella* has not been in routine use.

Several rapid detection methods have been developed over the past few years, such as enzyme-linked immunosorbent assay (ELISA) [11]. ELISA is based on the specific recognition of the antigen by antibodies and is measured with the aid of an enzyme–substrate reaction. Several different ELISA methods have been developed including competitive ELISA [12], PCR-ELISA [13] and Dot-ELISA [14, 15]. These ELISA methods are considered highly sensitive, and provide specific and rapid screening of a large number of samples for the presence of *Salmonella*. However, a disadvantage of the ELISA method is that it requires considerable amounts of antigen to be used for detection. Some research has reported that the detection sensitivity of ELISA was $10^5$ colony-forming unit (CFU) of *Salmonella spp.* per ml of culture [11]. Another effective method for the detection and identification of *Salmonella* is the polymerase chain reaction (PCR), which is based on isolating the bacteria and exponentially amplifying a DNA fragment or sequence of interest via enzymatic replication [5, 16, 17]. Real-time PCR offers the advantage of semi-quantification of the bacterial DNA and no post-PCR handling of the sample, thus reducing the risk of false-positive results [3, 4, 18, 19]. Although PCR and its modifications may detect *Salmonella* within a relatively short time, issues remain such as primer design and PCR-inhibitory effects of complex food matrices that make PCR detection of *Salmonella* in food far from being a routine procedure [4, 20]. Electrochemical biosensing has also been listed as one of the

 © 2008 IOP Publishing Ltd Printed in the UK

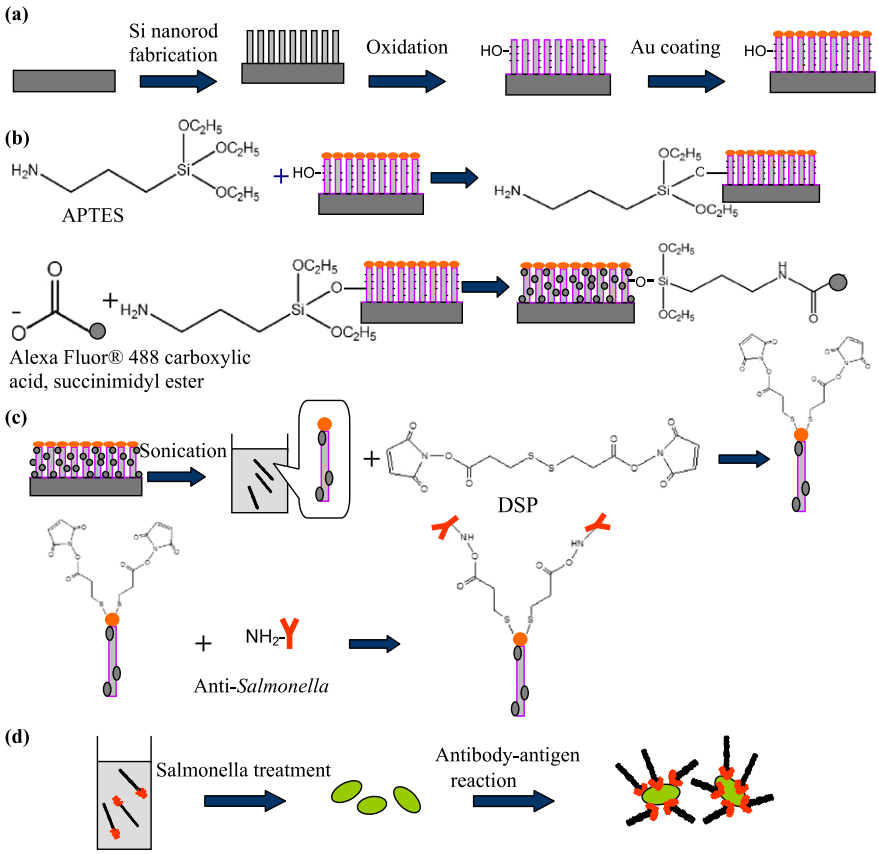


**Figure 1.** Process flow for the *Salmonella* detection by bio-functionalized Au/Si nanorods. (a) Au/Si nanorod fabrication; (b) dye immobilization onto the Si nanorods; (c) antibody conjugation onto the Au tip; (d) *Salmonella* detection via the antibody–antigen reaction.

fastest and most sensitive methods for *Salmonella* detection. The tested micro-organisms including *Salmonella* exhibited a different antibiotic susceptibility profile, which suggested the possibility of bacteria differentiation [21]. *In situ* monitoring of *Salmonella typhimurium* was developed by measuring the cathodic peak current of oxygen during bacterial proliferation with an electrochemical voltammetric analyzer [22].

Recently, highly sensitive sensors based on nanostructures and their unique physical or chemical properties have emerged and have shown great potential for pathogen detection. Some of these methods include detections by luminescence using quantum dots [23, 24], localized surface plasmon resonance of metallic nanoparticles [25], enhanced fluorescence [26], dye immobilized nanoparticles [27, 28], or Raman reporter molecule immobilized metallic nanoparticles [29]. All the nanostructures used for the biosensing applications have two characteristics. First, they contain certain recognition mechanisms specified to the analyte, for example, antibodies or enzymes. Second, they are able to generate a distinguishing signal from the analyte and this signal could be generated by the nanostructures themselves or produced by signaling molecules immobilized or contained in the nanostructures. For single component nanostructures, it can be difficult to immobilize the recognition molecules and signaling molecules simultaneously. Hetero-nanostructure provides a promising platform to solve this problem. Thus, different functional molecules can be immobilized to the different components of the hetero-nanostructure to enhance selectivity and specificity of detection. In this study, we show that Au/Si 'matchstick' nanorods used as a scaffold can be functionalized for conjugation with anti-*Salmonella* antibodies and a fluorescence dye (Alexa488) to rapidly and sensitively detect *Salmonella*.

## 2. Experimental methods

Silicon wafers (Montco Silicon Technologies, Inc.) were used as a substrate for the silicon (Si) nanorod growth. A gold (Au) target for the SPI-MODULE™ Sputter Coater was purchased from SPI supplies (Structure Probe, Inc.). Fluorescent dye, Alexa Fluor® 488, a carboxylic acid succinimidyl ester, was purchased from Invitrogen (Carlsbad, California). Unlabeled anti-*Salmonella* and killed *Salmonella* (*Salmonella typhimurium* strain) were obtained from Kirkegaard & Perry Laboratories, Inc. (KPL, Gaithersburg, MD). 3-Aminopropyltriethoxysilane (APTES) and Dithiobis-succinimidyl propionate (DSP) were from Sigma-Aldrich (St Louis, MO) and Pierce Chemical (Rockford, IL), respectively.

Au/Si hetero-structured nanorod-based *Salmonella* detection is facilitated by the enhanced fluorescence signal elicited during the binding of *Salmonella* to the anti-*Salmonella* antibodies conjugated to the nanorods. The method is illustrated in

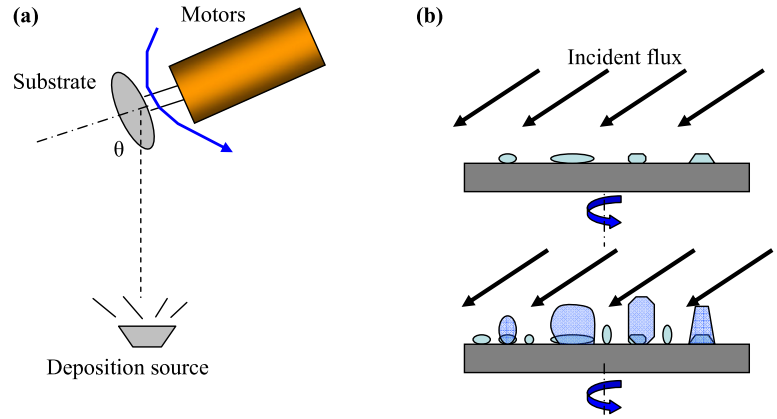


**Figure 2.** (a) A schematic diagram of the glancing angle deposition setup; (b) the shadowing effect.

figure 1. The vertically aligned Si nanorods are fabricated on the Si substrate and the subsequent oxidation process provides the hydroxyl groups on the nanorod surfaces. Then, a thin layer of Au is sputter-coated onto the nanorods (figure 1(a)). Using APTES, the silica surface is silanized with amine groups, which form the peptide bond with the amine-reactive carboxylic groups in the Alexa488-succinimide dye (figure 1(b)). To immobilize antibodies onto the nanorods, a DSP crosslinker will chemisorb to the Au surface by breaking the disulfide bond and conjugation of the anti-*Salmonella* antibody to Au is achieved by releasing of the *N*-hydroxysuccinimide, leaving groups via the primary amines (figure 1(c)). For detection, *Salmonella* can be fixed, reacted with the functionalized hetero-structured nanorods, and detected through signaling mediated by multiple Alexa488 dye molecules bound on the Si nanorods, and generate intense fluorescence signals providing detection of the bound *Salmonella* (figure 1(d)).

The Si nanorods were fabricated by the glancing angle deposition (GLAD) method based on a physical vapor deposition technique [30, 31]. The basic deposition setup is shown in figure 2(a). Nanorod growth is carried out in a high vacuum chamber. Inside the chamber, the collimated evaporation beam is incident on the substrate surface with an incident angle $\theta$ which is normally larger than 75°. The substrate is manipulated by two stepper motors: one motor controls the incident angle $\theta$ and another motor controls the azimuthal rotation of the substrate. A geometric shadowing effect is the main mechanism of GLAD (figure 2(b)). During the deposition, initially there are some nucleated islands formed on the substrate. Those islands serve as the shadowing centers. The taller islands receive more vapor atoms and grow into nanorods. The azimuthal rotation of the substrate makes all the nanorods grow vertically to the surface of the substrate. In this study, during the deposition for Si nanorods, the incident angle was fixed at 86°; the deposition rate (0.4 nm $s^{-1}$) was monitored by the quartz crystal microbalance which was facing directly down towards the vapor source, while the substrate azimuthal rotation speed (0.05–0.25 Hz) was controlled by a computer.

To oxidize the Si surface, Si nanorods were treated by SPI Plasma-Prep™ II Plasma Etcher (SPI supplies) with pure oxygen for 10 min. Following this, a thin layer of Au was sputtered onto the top of the Si nanorods by a SPI-MODULE™ sputter coater system (SPI supplies). In this coater chamber, the substrate of the Si nanorods was placed facing down towards the Au target at a distance of 4 cm. The Au thickness was approximately monitored by the coating time.

After Au coating, 2% APTES in acetone, the coupling agent, was annealed to the hydroxyl groups on the oxidized Si nanorods (45 °C, overnight). The excess reagent was separated from the Si nanorods by washing three times with acetone. Alexa488-succinimide ester was applied to the APTES/Si nanorods at room temperature for 1 h and then transferred to 4 °C overnight. The dye ester attached to the Si nanorods via the primary amine supplied by the APTES and excess dye was washed off by deionized (DI) water. The Alexa488 dye immobilized on the Au-coated Si nanorods (DNRs, Au/Si nanorod/Alexa488) were air dried and dispersed in acetone using BRANSON MODEL 2510 ultrasonic cleaner (Kell-Strom, Wethersfield, CT). The sonication time was 1–2 h. After sonication, the original substrate had a shining silicon surface. Approximately 80–90% of the nanorods came off the surface and dispersed in the acetone uniformly.

The DNRs were centrifuged (Centronix microcentrifuge, National Labnet Co.) to the bottom of the glass vial. Then the supernatant was removed, and the DNRs were air dried. A 5 mg $ml^{-1}$ solution of DSP in acetone was added to the DNRs and incubated for 30 min at room temperature. The DNRs/acetone suspension was centrifuged and the supernatant removed. Fresh acetone was added, and the DNRs were re-suspended by vortexing. By repeating this process, the DNRs were washed using acetone at least three times. Following the last wash, 100 $\mu$g $ml^{-1}$ anti-*Salmonella* in phosphate buffered saline buffer (FA Buffer, pH 7.2, for use with fluorescent-antibody reagents, BD, Franklin Lakes, NJ) was added to the dried DNRs, and the DNRs were re-suspended in FA buffer by sonication. After 2 h incubation at room temperature, the DNRs were transferred to the refrigerator overnight. The anti-*Salmonella*-DNRs were then washed with FA buffer by centrifuge several times to remove unbound anti-*Salmonella* antibody. The final concentration of the anti-*Salmonella*-DNR suspension was estimated to be $\sim 3.6 \times 10^9$ nanorods $ml^{-1}$.

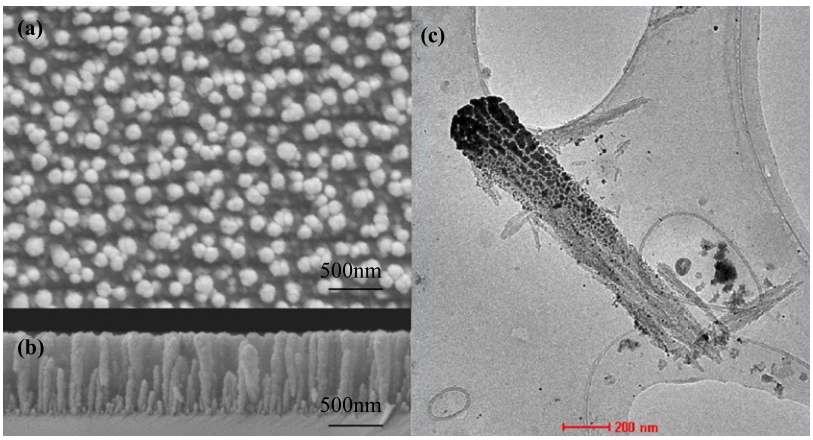


**Figure 3.** Images of Au-coated Si nanorods with 2000 nm normal film thickness in the normal direction. (a) Top-view SEM image; (b) cross section SEM image; (c) TEM image.

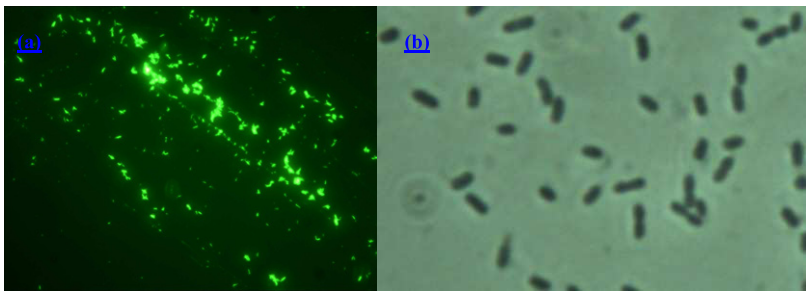


**Figure 4.** (a) Fluorescence image of Au/Si nanorods/Alexa488 (DNRs). (b) *Salmonella* observed under the optical microscope.

The microscope slides (Gold Seal, Portsmouth, NH) were cleaned using Piranah solution (one part hydrogen peroxide and four parts sulfuric acid) and rinsed with DI water. The slides were dried in nitrogen and prepared for use. A 2 $\mu$l suspension of $10^9$ cfu ml$^{-1}$ *Salmonella* bacterial ($2 \times 10^6$ bacteria in total) was loaded onto the cleaned microscope slide and allowed to air dry. To fix the *Salmonella* antigen, the slide was placed in 95% ethanol for 1 min, removed, and allowed to air dry.

The DNR suspension was used as the negative control. In this case, both the anti-*Salmonella*-DNR suspension and the DNR suspension (50 $\mu$l) were applied to the fixed bacteria for 2 h under room temperature. The slides were maintained in a humidified atmosphere to avoid the suspensions drying out during the incubation. After the incubation, the slides were washed by 0.05% Tween/FA buffer three times and once with DI water.

## 3. Results and discussion

A scanning electron microscope (SEM) was used to determine the dimensions of the Si nanorods (figures 3(a) and (b)). The SEM shows the top-view and cross-section images of the Au/Si nanorods deposited as a 2000 nm normal film thickness on the substrate. The nanorods have a needle shape, and by estimation, the top diameter, the bottom diameter, and the length of the nanorod were 150, 60 and 900 nm, respectively. The density of Si nanorods was estimated to be 20 $\mu$m$^{-2}$. The high aspect ratio of the nanorods can accommodate more dye molecules than the flat surface (see supplementary information figure S1 available at stacks.iop.org/Nano/19/155502). By assuming that the Si nanorod takes a cylindrical shape, we calculated the surface area ratio of the nanorod surface to the flat surface as 9.48.

A gold layer with a thickness of 5 nm was sputtered on the Si nanorods. As shown in the transmission electron microscopy (TEM) image (figure 3(c)), the black areas are indicative of gold coating on the Si nanorods. Most of the gold was distributed on the top of the Si nanorod, however some gold clusters were deposited on the side wall of the Si nanorod, giving the appearance of a 'matchstick'. Using TEM, the gold particle size was estimated as 1–3 nm. Since the sputtering method used is based on argon plasma, and the directionality of the incident vapor has a wide angular distribution, side wall Au deposition is expected.

In the process of dye immobilization, the Alexa488-succinimide dye bound the amine group provided by APTES on the Si nanorods. To evaluate the effect of the immobilization, a 10 $\mu$l drop of Au–Si nanorods/Alexa488 suspension was sandwiched between the microscope slide and a cover slide and observed on a fluorescence microscope (Olympus BX60). The fluorescent image of the DNR was observed under the 488 nm excitation and 100× objective as shown in figure 4(a). The results show strong green

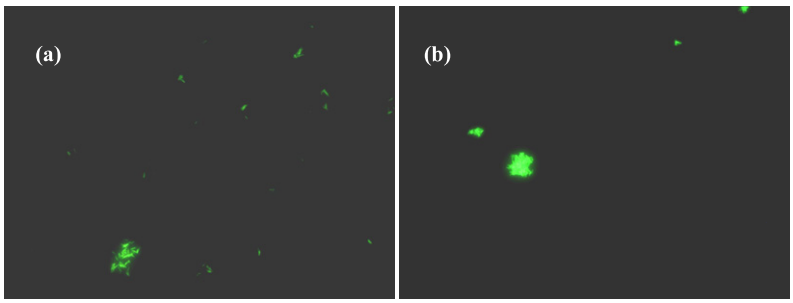


**Figure 5.** Fluorescence images of (a) anti-*Salmonella*-DNR and (b) DNR treated *Salmonella* detection slides.

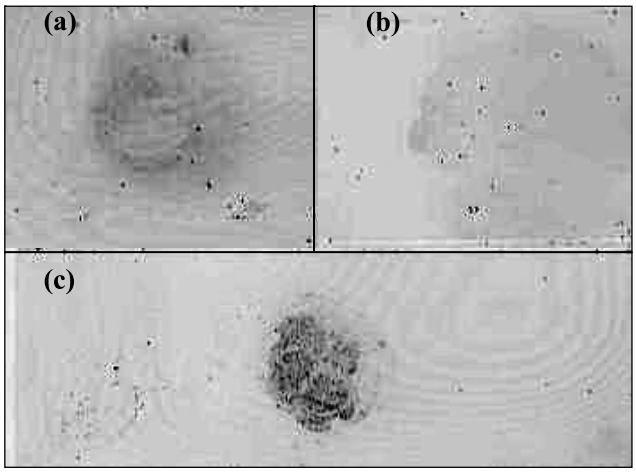


**Figure 6.** Fluorescence scans for *Salmonella* slides by a Typhoon scanner. (a) 50 $\mu$l anti-*Salmonella*-DNR with a 2% BSA treated slide; (b) 50 $\mu$l DNR with a 2% BSA treated slide; (c) 50 $\mu$l DNR (no BSA treatment) treated slide.

fluorescence emitted from the nanorods, demonstrating that the Alexa488 was successfully immobilized onto the Si nanorods (see supplementary information figure S2 available at stacks.iop.org/Nano/19/155502).

To evaluate the efficacy of the hetero-nanostructured biosensor for detection of *Salmonella*, a 2 $\mu$l suspension of $10^9$ cfu ml$^{-1}$ *Salmonella* bacteria ($2 \times 10^6$ bacteria in total) was fixed onto the detection slides, incubated with the anti-*Salmonella*-DNR suspension and the DNR suspension, and washed as described in section 2. Before the incubation, the *Salmonella* were observed by microscopy (figure 4(b)) and they appeared as gray, thick elongated particles. After the washes, the slides were transferred to the fluorescence microscope. Figure 5 showed the fluorescence images taken from the anti-*Salmonella*-DNR treated slide and control DNR treated slide. The anti-*Salmonella*-DNR treated slide exhibited strong fluorescent signaling compared to the control DNR treated slide (figure 5), although some autofluorescence was observable in the control. This may be due to non-specific interaction of the *Salmonella* specimen with the gold surface.

To block non-specific reactivity on the gold surface, bovine serum albumin (BSA) solution was added in both the anti-*Salmonella*-DNR suspension and the DNR suspension. A 2% BSA blocking step effectively reduced or eliminated most of the non-specific binding. Using this blocking procedure, the anti-*Salmonella*-DNR treated slide yielded strong visible detection (Typhoon Imager, Amersham) while the DNR treated slide showed almost no detectable signal (figures 6(a) and (b)). As a comparison, a non-BSA treated DNR suspension was also applied to a *Salmonella* slide, and its fluorescence scanned image is shown in figure 6(c).

The slides, as shown in figures 6(a) and (b), were also evaluated by a fluorescence microscope under an excitation laser with a wavelength of 488 nm and under the white light sequentially for the same location. Figures 7(a) and (b) show the anti-*Salmonella*-DNR treated *Salmonella* slide under laser excitation and white light, respectively. As shown in figure 7(a), intense green spots indicating positive identification were observed on the sample that corresponds to anti-*Salmonella*-DNRs. At the same location, under white light, there are also particles and aggregates observed in the image (figure 7(b)). Comparing figure 7(a) to (b), there appears to be mostly a one-to-one correspondence between the particles or aggregates. To further illustrate this relationship, areas of the image in figures 7(a) and (b) have been enlarged and presented in the insets. The inset in figure 7(a) shows 6–7 fluorescent particles with different orientations, while the corresponding inset in figure 7(b) shows 11–12 particles. However, the particles have two different appearances, i.e. gray, thick elongated particles and blue, thin longer particles. From the location and orientation of the particles (figure 7(a)), it may be concluded that these blue longer particles correspond to the fluorescence particles, i.e. they are anti-*Salmonella*-DNRs, while the gray, thicker particles are *Salmonella* bacteria, similar to those shown in figure 4(b). From the relative locations of the anti-*Salmonella*-DNRs and the *Salmonella* bacteria, one may conclude that each *Salmonella* bacterium binds with one anti-*Salmonella*-DNR. Although only one hetero-structured nanorod appears to capture one *Salmonella* bacterium, the fluorescence signal generated from the DNRs is strong enough for us to obtain single bacterium detection. It may be possible to increase the nanorod concentration in future studies in order to potentially improve the detection signal, i.e. one cell capturing two or more nanorods. For the negative control, we only found very few fluorescent spots, as shown in figure 7(c), which demonstrates the specificity of this novel biosensor.

Though the detection limit and the specificity are under investigation, the results still show that multifunctional hetero-nanorods have promising potential for *Salmonella* detection. The Au/Si hetero-nanostructure based biosensor has several advantages in biological detection, particularly the potential

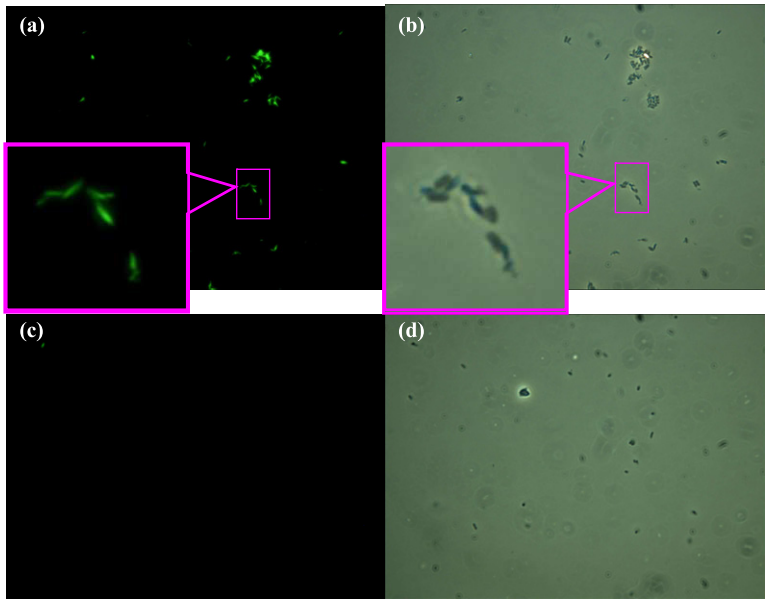


**Figure 7.** Images for *Salmonella* detection. (a) 50 $\mu$l anti-*Salmonella*-DNR with a 2% BSA treated slide under fluorescence excitation (488 nm excitation); (b) 50 $\mu$l anti-*Salmonella*-DNR with a 2% BSA treated slide under white light; (c) 50 $\mu$l DNR with a 2% BSA treated slide under fluorescence excitation (488 nm excitation); (d) 50 $\mu$l DNR with a 2% BSA treated slide under white light. The insets in figures (a) and (b) are enlargements of the corresponding locations in the two images.

sensitivity to detect a single bacterium. It may be possible to further enhance detection, by improving Au layering on the nanorods, possibly by using a thermal evaporation method. Another beauty of this method is that, by varying the fluorescence dyes and antibodies, this biosensor technique can be used as a platform technique to detect other pathogens, or a mixture of pathogens. For example, by changing the anti-*Salmonella* antibody to the *Respiratory Syncytial Virus* (RSV) antibody, this nanorod-based biosensor has also been successfully used to detect RSV infected cells. The RSV antibody (131-2A) was conjugated to Au/Si nanorod/Alexa488 nanostructures before they were sonicated into 3 ml PBS buffer (see supplementary information figure S3 available at stacks.iop.org/Nano/19/155502). During the sonication, ice was added in the tray to keep the temperature low. Then both the 1/2 diluted and 1/4 diluted nanorod suspensions were added to the RSV infected cells and uninfected cells. The uninfected cells were used as the control. After the incubation and further rinses, the cells were scanned by the Typhoon fluorescence scanner (532 nm excitation/526 nm short pass emission filter), and the results are given in figure 8. The uninfected cells do not show any significant fluorescence signals while the infected cells show different fluorescence intensities for different diluted nanorod suspensions. This result indicates that the fluorescence signal was detected as the RSV antibodies were specifically bound by the RSV antigen. All the results shown here demonstrate a new, novel and potentially very rapid means to sensitively detect important pathogens.

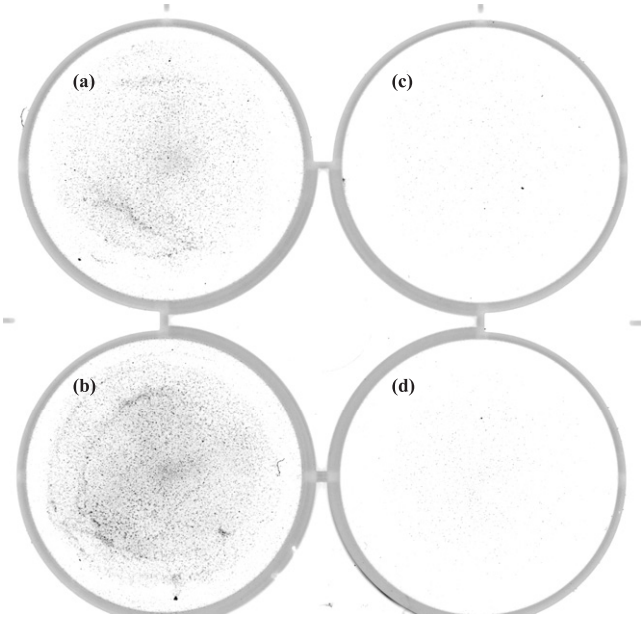


**Figure 8.** *Respiratory syncytial virus* (RSV) infected cells detected by a Au/Si hetero-nanorod-based biosensor. (a) A 1/4 bio-functional nanorod dilution was applied to the RSV infected cells; (b) a 1/2 bio-functional nanorod dilution was applied to the RSV infected cells; (c) a 1/4 bio-functional nanorod dilution was applied to the uninfected cells; (d) a 1/2 bio-functional nanorods dilution was applied to the uninfected cells.

## 4. Conclusions

A novel Au/Si hetero-structured nanorod-based detection method for *Salmonella* has been developed. A single bacterium was captured by the antibodies conjugated on the Au and detected by thousands of dye molecules immobilized on the Si nanorods. This fluorescence-based detection method provides a platform technology that may be applied to detection strategies for other pathogens as, in principle, the antibody used for capture can be substituted as required.

For example, we have changed the anti-*Salmonella* antibody to RSV antibodies, and have successfully detected the RSV infected cells. Additionally, the fluorescent detection dye can also be replaced by other types of dyes or potentially quantum dots that may allow for multiplex detection. In principle, other nano-building blocks, such as spherical silica nanoparticles or the commercially available fluorescent silica nanoparticles, after partially coating with Au, can also be used as the same detection biomarkers, though other techniques will be needed to deal with the Au coating and the antibody conjugation. In addition, this hetero-nanostructure based detection method could expand the applications in many related fields such as pathogen detection, drug delivery, and bio-engineering.

## Acknowledgments

We are grateful for the support from NSF under contract ECS-0404066 and KFRI under the ARS agreement 58-6612-6-089F. The authors thank Justin Abell for proof-reading the manuscript.

## References

[1] Munson T E *et al* 1976 *Appl. Environ. Microbiol.* **31** 514
[2] Walker R L *et al* 2001 *Int. J. Food Microbiol.* **67** 123
[3] Uyttendaele M, Vanwildemeersch K and Debevere J 2003 *Lett. Appl. Microbiol.* **37** 386
[4] Hein I *et al* 2006 *J. Microbiol. Methods* **66** 538
[5] Myint M S *et al* 2006 *Food Microbiol.* **23** 599
[6] Aleixo J A G and Swaminathan B 1988 *J. Immunoassay* **9** 83
[7] McClelland R G and Pinder A C 1994 *J. Appl. Bacteriol.* **77** 440
[8] Minet J *et al* 1991 *Water Sci. Technol.* **24** 373
[9] Mohr H K, Trenk H L and Yeterian M 1974 *Appl. Microbiol.* **27** 324
[10] Thomason B M 1971 *Appl. Microbiol.* **22** 1064
[11] Tian H Z *et al* 1996 *J. Food Prot.* **59** 1158
[12] Tan S, Gyles C L and Wilkie B N 1997 *Vet. Microbiol.* **56** 79
[13] Scheu P *et al* 1998 *Food Biotechnol.* **12** 1
[14] Rahman H 1999 *Indian J. Med. Res.* **110** 47
[15] Tapchaisri P *et al* 1999 *Asian Pac. J. Allergy Immunol.* **17** 41
[16] Correa A A *et al* 2006 *J. Food Quality* **29** 458
[17] Trafny E A, Kozlowska K and Szpakowska M 2006 *Lett. Appl. Microbiol.* **43** 673
[18] Wang X W, Jothikumar N and Griffiths M W 2004 *J. Food Prot.* **67** 189
[19] Notzon A, Helmuth R and Bauer J 2006 *J. Food Prot.* **69** 2896
[20] Gunaydin E, Eyigor A and Carli K T 2007 *Lett. Appl. Microbiol.* **44** 24
[21] Morales M D *et al* 2007 *Analyst* **132** 572
[22] Ruan C M, Yang L J and Li Y B 2002 *J. Electroanal. Chem.* **519** 33
[23] Edgar R *et al* 2006 *Proc. Natl Acad. Sci. USA* **103** 4841
[24] Yang L J and Li Y B 2005 *J. Food Prot.* **68** 1241
[25] Thomas E *et al* 2006 *J. Immunol. Methods* **315** 68
[26] Henry R *et al* 2004 *Anal. Biochem.* **334** 1
[27] Agrawal A *et al* 2005 *J. Virol.* **79** 8625
[28] Valanne A *et al* 2005 *J. Virol. Methods* **129** 83
[29] Wang W, Ruan C M and Gu B H 2006 *Anal. Chim. Acta* **567** 121
[30] Robbie K and Brett M J 1997 *J. Vac. Sci. Technol.* A **15** 1460
[31] Zhao Y P *et al* 2002 *Nano Lett.* **2** 351